$p27^{Kip1}$ expression inhibits glioblastoma growth, invasion, and tumor-induced neoangiogenesis

Monica Schiappacassi,[1] Francesca Lovat,[1] Vincenzo Canzonieri,[2] Barbara Belletti,[1] Stefania Berton,[1] Domenica Di Stefano,[3] Andrea Vecchione,[3] Alfonso Colombatti,[1,4,5] and Gustavo Baldassarre[1]

[1]Division of Experimental Oncology 2 and [2]Division of Pathology, Centro di Riferimento Oncologico, Istituto Nazionale Tumori, IRCCS, Aviano, Italy; [3]Division of Pathology, II Faculty of Medicine, University ''La Sapienza,'' Ospedale Santo Andrea, Rome, Italy; and [4]Dipartimento di Scienze e Tecnologie Biomediche and [5]MATI Center of Excellence, University of Udine, Udine, Italy

Abstract

The tumor suppressor gene *CDKN1B* encodes for a 27-kDa cyclin-dependent kinase inhibitory protein, $p27^{Kip1}$, which together with its well-established role in the inhibition of cell proliferation, displays additional activities in the control of gene transcription and cell motility. $p27^{Kip1}$ thus represents a good candidate for a gene therapy approach, especially in those cancers refractory to the conventional therapies, like human glioblastoma. Here, we show that overexpression of $p27^{Kip1}$ in glioblastoma cell lines induced cell cycle arrest and inhibition of cell motility through extracellular matrix substrates. The use of adenoviral vectors in the treatment of glioblastoma *in vivo* showed that $p27^{Kip1}$ was able to block not only cancer cell growth but also local invasion and tumor-induced neoangiogenesis. The latter effect was due to the ability of p27 to impair both endothelial cell growth and motility, thus preventing proper vessel formation in the tumor. The block of neoangiogenesis depended on cytoplasmic $p27^{Kip1}$ antimigratory activity and was linked to its ability to bind to and inhibit the microtubule-destabilizing protein stathmin. Our work provides the first evidence that a successful $p27^{Kip1}$-based gene therapy is linked to tumor microenvironment modification, thus opening new perspectives to the use of gene therapy approaches for the treatment of refractory cancers. [Mol Cancer Ther 2008;7(5):1164–75]

Introduction

$p27^{Kip1}$ (hereafter p27) belongs to the Cip/Kip family of cyclin-dependent kinase inhibitors that binds and inhibits, although with a different threshold, all the cyclin/cyclin-dependent kinase complexes, thus often referred to as an universal cyclin-dependent kinase inhibitor (1). It has been extensively shown that for the proper control of cell proliferation p27 has to bind and regulate the cyclin-dependent kinase nuclear activity, because its displacement in the cytoplasm results in loss of cell cycle inhibition (2–4). Recently, several research groups reached the conclusion that diverse biological functions of p27 are correlated to its cytoplasmic localization. Among these studies, the role of p27 on cell motility has become an interesting matter of scientific literature (5–9). We recently reported that cytoplasmic p27 interacts with and inhibits the microtubule-destabilizing protein stathmin, thus inhibiting sarcoma cell motility through extracellular matrix (ECM) substrates (5).

Cell cycle deregulation is a hallmark of cancer; in particular, reduced expression of p27 has been extensively observed in human cancers and often its low levels are associated to a worse prognosis (10, 11). Moreover, lack of p27 has also been linked to increased invasion and metastasis formation in several types of human tumors (12–17). Few studies have addressed systematically the effect of p27 cytoplasmic localization in tumor progression. The largest one done in breast carcinomas showed that patients with high cytoplasmic expression of p27 had a better survival with respect to patients with low expression, although the best prognosis was found in patients with high nuclear p27 staining (18). In malignant glioblastoma, low p27 expression levels have been often associated with poor prognosis and increased proliferation (19–22). Smaller studies did not confirm this correlation (23, 24), a discrepancy that could be due to the heterogeneity of gliomas (25) or to the different cutoff used to evaluate p27-positive cells within the tumors. Malignant glioblastoma represents an ideal candidate for local gene therapy approaches, because it prevalently invades the surrounding parenchyma rarely forming distant metastasis and because it is almost invariably resistant to current therapeutic approaches. Being p27 an attractive target for new therapeutic opportunity in cancers (3, 10), we explored the effects of p27 expression using a tetracycline-inducible adenoviral system *in vitro* and *in vivo* gene therapy experiments on glioblastoma cells.

Received 10/1/07; revised 1/18/08; accepted 1/21/08.

Grant support: Association for International Cancer Research (G. Baldassarre) and partially Associazione Italiana Ricerca sul Cancro (G. Baldassarre and A. Vecchione); Associazione Italiano Ricerca sul Cancro fellowship (F. Lovat) and Federazione Italiana Ricerca sul Cancro fellowship (S. Berton).

The costs of publication of this article were defrayed in part by the payment of page charges. This article must therefore be hereby marked *advertisement* in accordance with 18 U.S.C. Section 1734 solely to indicate this fact.

Note: M. Schiappacassi and F. Lovat contributed equally to this work.

Requests for reprints: Gustavo Baldassarre, Division of Experimental Oncology 2, Centro di Riferimento Oncologico, Istituto Nazionale Tumori, IRCCS, Via Franco Gallini, 2 33081 Aviano, Italy. Phone: 39-434-659-233; Fax: 39-434-659-428. E-mail: gbaldassarre@cro.it

doi:10.1158/1535-7163.MCT-07-2154

Materials and Methods

Tissue Samples

A total of eight brain tumors were collected and diagnosed at University La Sapienza Rome according to the WHO criteria. For immunohistochemical staining, four glioblastoma multiformes (grade 4) and four anaplastic astrocytomas (grade 3) were evaluated using an anti-human p27 antibody from DAKO.

Cell Lines

Human embryonic kidney cells [HEK 293, ATCC CRL-1573, and 293 H (Life Technologies)] were used to generate recombinant adenovirus. Human malignant glioma cell lines U87MG, U138MG, T98G, U251MG, SF268, SBN75, U373, SF539, SF295, and SBN19 were kindly provided by Prof. A. Fusco (Università Federico II di Napoli) and maintained in RPMI 1640 supplemented with 10% heat-inactivated fetal bovine serum.

Human umbilical vein endothelial cells (HUVEC) were isolated from human umbilical cords as described previously (26). Cells were grown on 1% gelatin-coated plates in M199 supplemented with 20% fetal bovine serum, 1% penicillin/streptomycin, and bovine brain extract (0.5%).

Preparation of Cell Lysates, Immunoblotting, and Immunoprecipitation

Total protein and nuclear/cytoplasmic extracts were prepared as reported previously (5). For immunoblotting, protein extracts were separated in 4% to 20% SDS-PAGE (Criterion Precast Gel; Bio-Rad) and transferred to nitrocellulose membranes (Amersham). Primary antibodies were from Transduction Laboratories (p27, CDK1, and CDK2), Santa Cruz Biotechnology (p27 C19, p27 N20, p27, CDK1, cyclin B1, vinculin, Akt, and c-Abl), Sigma (stathmin and α-tubulin), Cell Signaling (pS473Akt), and Upstate Biotechnology (histone H1).

Membranes were incubated with primary antibodies according to experimental design and then with horseradish peroxidase–conjugated (ECL Kit; Amersham) or Alexa-conjugated secondary antibodies (Odyssey Infrared Detection System; Li-Cor). Immunoprecipitation experiments were done using 0.5/1.0 mg total lysate and protein A/G-Sepharose (Amersham). True Blot reagent (e-Bioscience) was used as secondary anti-mouse or anti-rabbit antibody.

Animal Experiments

Human glioblastoma xenografts were established by s.c. injection of 10^7 U87MG cells into female athymic nude mice (Harlan; 8 weeks old). When tumors were ~40 to 60 mm^3 (~15 days from injection), the animals (10 mice per group of treatment) were randomly divided into groups according to experimental design and intratumoral injections were done with 2×10^9 total infectious units (AdTRE/AdTet-ON, 80:40) and repeated five times every 2 days. Tumor size was measured with a caliper three

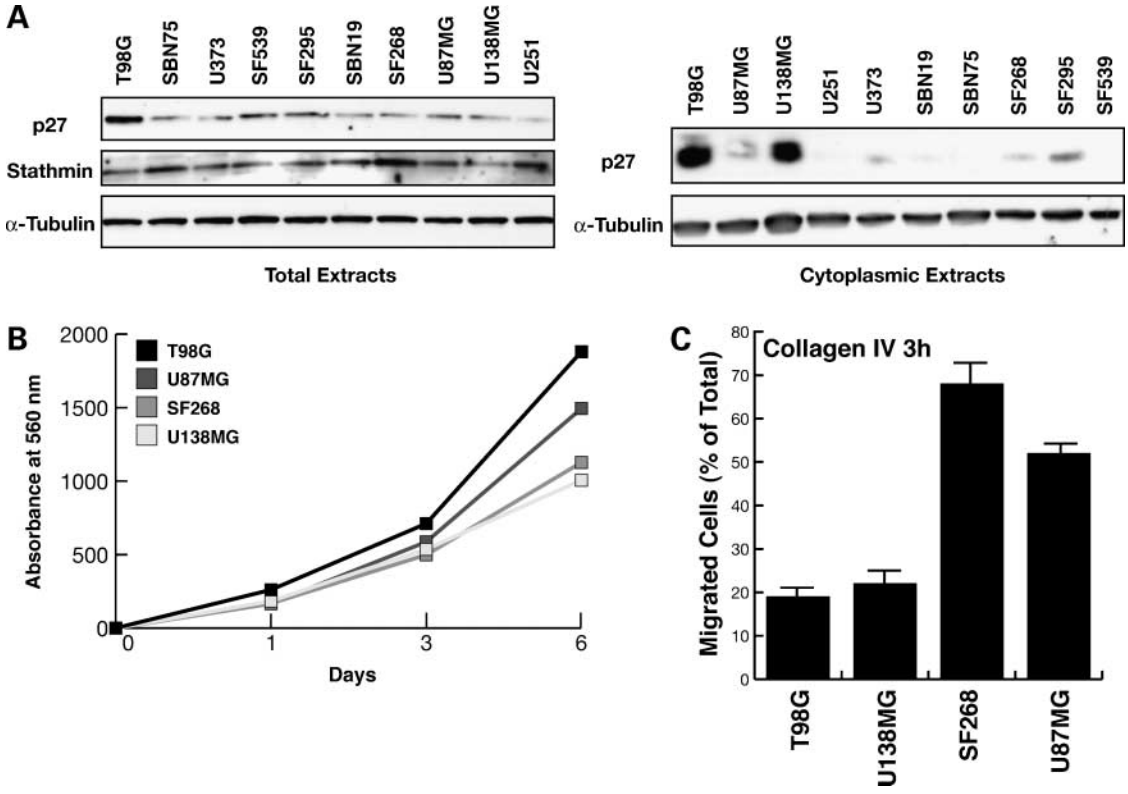

Figure 1. Cytoplasmic p27 levels correlated with migration ability of glioblastoma cell lines. **A,** Western blot analysis of p27 and stathmin expression in total and cytoplasmic cell extracts of different glioblastoma cell lines. α-Tubulin was used as loading control. **B,** MTT assay used to evaluate cell proliferation of the indicated cell lines. **C,** migration assay of the indicated cell lines through collagen IV–coated membranes. Results are expressed as percentage of migrated cells. Mean ± SD of two independent experiments each done in duplicate.

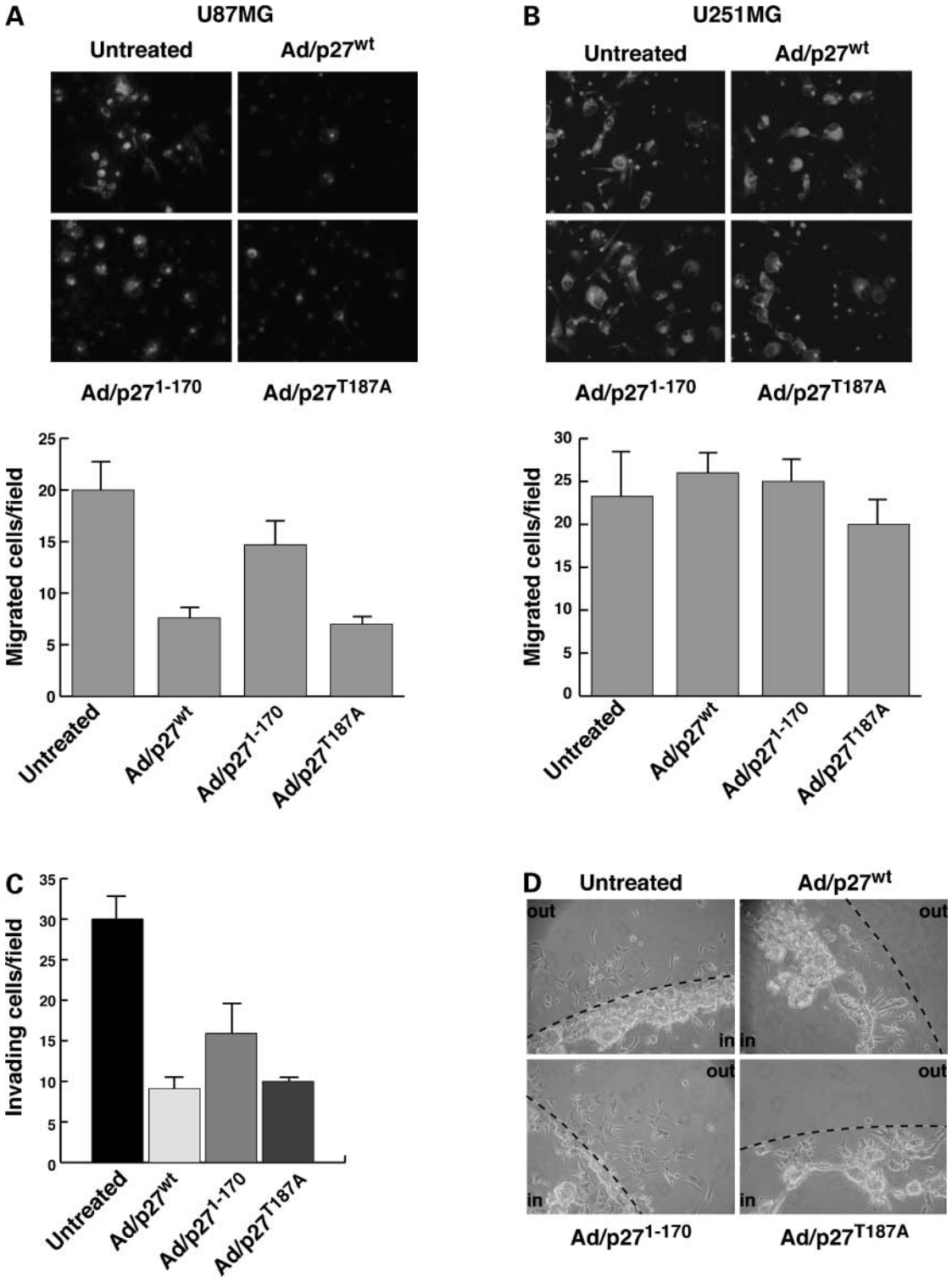

Figure 2. Overexpression of p27 impairs U87 MG cell motility. U87MG (**A**) and U251MG (**B**) cells were transduced with the indicated AdTRE and 48 h post-transduction seeded on fibronectin-coated fluorobloks and allow to migrate for 6 to 8 h. *Top,* representative fields of migrated U87MG (**A**) and U251MG (**B**) cells treated as indicated; *bottom,* quantification of migrated U87MG (**A**) and U251MG (**B**). Mean of at least three independent experiments done in duplicate. **C,** quantification of invading U87MG cells transduced as indicated, plated on Matrigel-coated fluorobloks, and allowed to invade for 48 h. Data are expressed as invading cells per field. Mean ± SD of three independent experiments done in duplicate. **D,** Matrigel evasion assay of U87MG cells included in Matrigel drops and incubated at 37°C for 5 d. Representative microphotographs are shown (magnification, ×100) showing that only control and $p27^{1-170}$-transduced cells were able to efficiently evade from Matrigel drops.

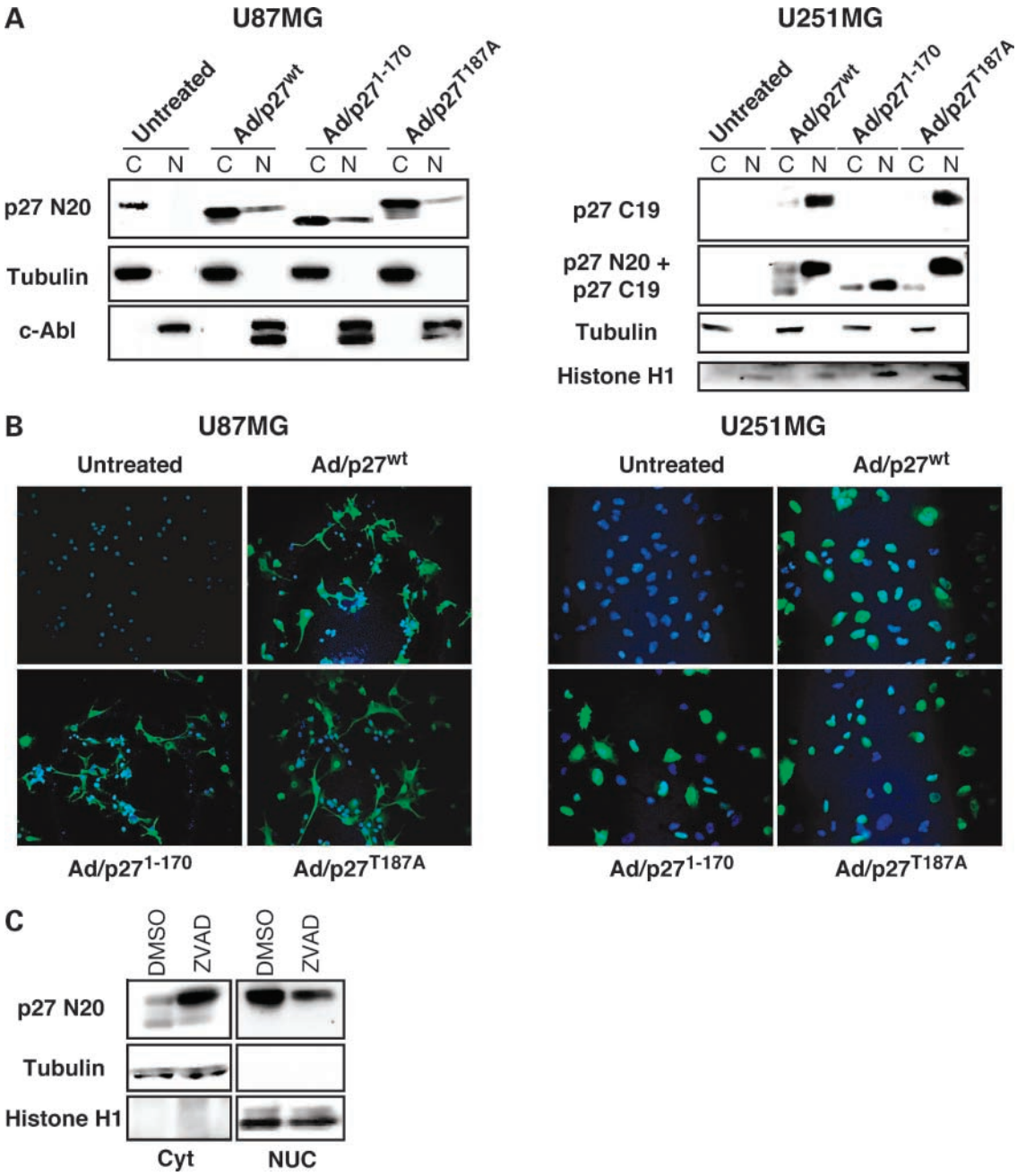

Figure 3. Different subcellular localization of p27 in U87MG and U251MG glioblastoma cells. **A,** Western blot analysis of p27 expression in cytoplasmic/nuclear extracts of U87MG and U251MG cells transduced as indicated and plated on fibronectin for 1 h. α-Tubulin was used as control for cytoplasmic fractions and c-Abl or histone H1 as controls for nuclear fractions. The p27 N20 antibody is directed against an epitope present at the NH_2-terminal part of the protein, whereas the C19 antibody recognized an epitope present at the COOH terminus of the protein. Accordingly, the N20, but not the C19, antibody recognized the $p27^{1-170}$ mutant. **B,** immunofluorescence analysis of glioblastoma adhered to fibronectin for 1 h confirmed that p27 had a predominant cytoplasmic localization in U87MG cells and an enriched nuclear localization in U251MG cells. *Blue,* Hoechst nuclear staining. **C,** Western blot analysis of p27 expression in the nucleus and cytoplasm of U251MG cells transduced with AdTRE $p27^{WT}$ and then treated for 48 h with vehicle (DMSO) or with the caspase inhibitor Z-VAD-FMK (35 μmol/L; R&D Systems).

times weekly and volume was calculated as 0.5 × length × width^2. Unless differently indicated, animals were sacrificed after 15 days of treatment and tumor analysis was done.

In the tumor prevention models, 7×10^6 U87MG cells were transduced with 80:40 AdTRE/AdTet-ON and then harvested 48 h later. Cells were then washed, resuspended in DMEM without red phenol, and injected s.c. into nude

mice (8 mice per group of treatment). Animals were sacrificed after 25 days for tumor analysis. For *in vivo* induction of p27 expression, 2 days before cell injection and for all the course of the experiment, drinking water was supplemented with 1 mg/mL doxycycline and 2.5% (w/v) sucrose and changed every 2 days.

Histologic Evaluation and Determination of Microvessel Density on Xenograft Tumor Sections

Explanted tumors were formalin-fixed and included in paraffin. At least 10 sections per tumor stained with H&E were analyzed in blind by an expert pathologist to evaluate the presence of local invasion.

For microvessel density analysis, explanted tumors were included in OCT and frozen in liquid N_2. Sections were incubated with anti-mouse CD31 (PECAM) monoclonal antibody (1:20; BD PharMingen) and visualized via three-step staining procedure in combination of biotinylated polyclonal anti-rat Ig mouse-adsorbed (Vector Laboratories; 5 μg/mL), and streptavidin-horseradish peroxidase (Sigma; 1:400) using 3,3-diaminobenzidine as substrate. The slides were then counterstained with hematoxylin. The number and the length of $CD31^+$ vessels were calculated in blind using a Leica microscope coupled with the Leica IM software. Ten randomly selected fields per section and at

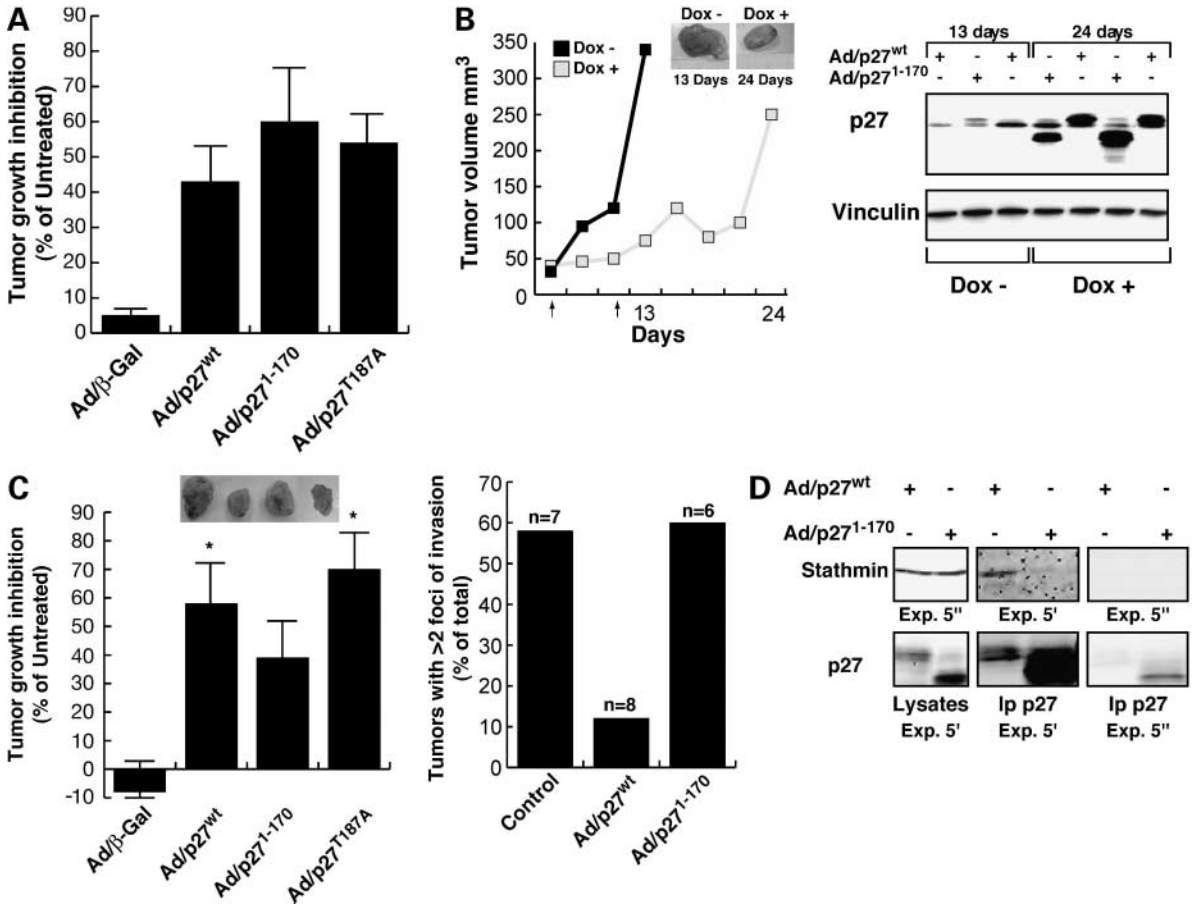

Figure 4. p27 impairs glioblastoma growth and invasion *in vivo*. **A,** U87MG cells transduced with the indicated AdTRE or left untreated were injected s.c. in nude mice fed with doxycycline and allowed to grow *in vivo* for 25 d. Mice were then sacrificed and tumor mass was evaluated. Data are expressed as percent of growth inhibition (that is, 50% represent the reduction to the half of the tumor mass expressed in grams) exerted by each AdTRE with respect to untreated tumors. In each group of treatment, six of eight animals were used. **B,** representative *in vivo* tumor growth of xenografts tumors treated with five intratumoral injection of AdTRE $p27^{wt}$ in mice fed with (*Dox+*) or without (*Dox-*) doxycycline in drinking water (*left*). *Inset,* typical images of the explanted tumors. *Arrows,* start and end of the treatment. Mice fed without doxycycline have been sacrificed earlier (13 d after the first intratumoral injection of the adenovirus) for humanitarian reasons. *Right,* Western blot analysis of p27 expression in tumor total protein lysates extracts from animals treated as described above and fed with (four different tumors) or without (three different tumors) doxycycline in drinking water. Vinculin was used as loading control. **C,** *left,* tumor growth inhibition exerted by AdTRE β-Gal, $p27^{wt}$, $p27^{1-170}$, and $p27^{T187A}$ intratumoral injection done as in **B** in animals fed with doxycycline. Mice were then sacrificed 15 d after the first adenovirus intratumoral injection. Percent of tumor growth inhibition was calculated on tumor mass expressed in grams as in **B**. Mean ± SD of 8 to 10 animals per group of treatment. *, $P < 0.05$, with respect to the AdTRE $p27^{1-170}$ treatment. *Right*, histologic evaluation of local invasion in explanted tumors treated as indicated. The percentage of tumors with more than two zones of local invasion is reported. The number of analyzed tumors per group of treatment is reported in the graph. **D,** expression of p27 and stathmin in whole-cell lysates (*left*) and p27-immunoprecipitated proteins (*middle* and *right*) from AdTRE $p27^{wt}$ and $p27^{1-170}$-treated tumors. Stathmin coprecipitated with overexpressed $p27^{wt}$ but not with $p27^{1-170}$. The exposure time is indicated under each panel.

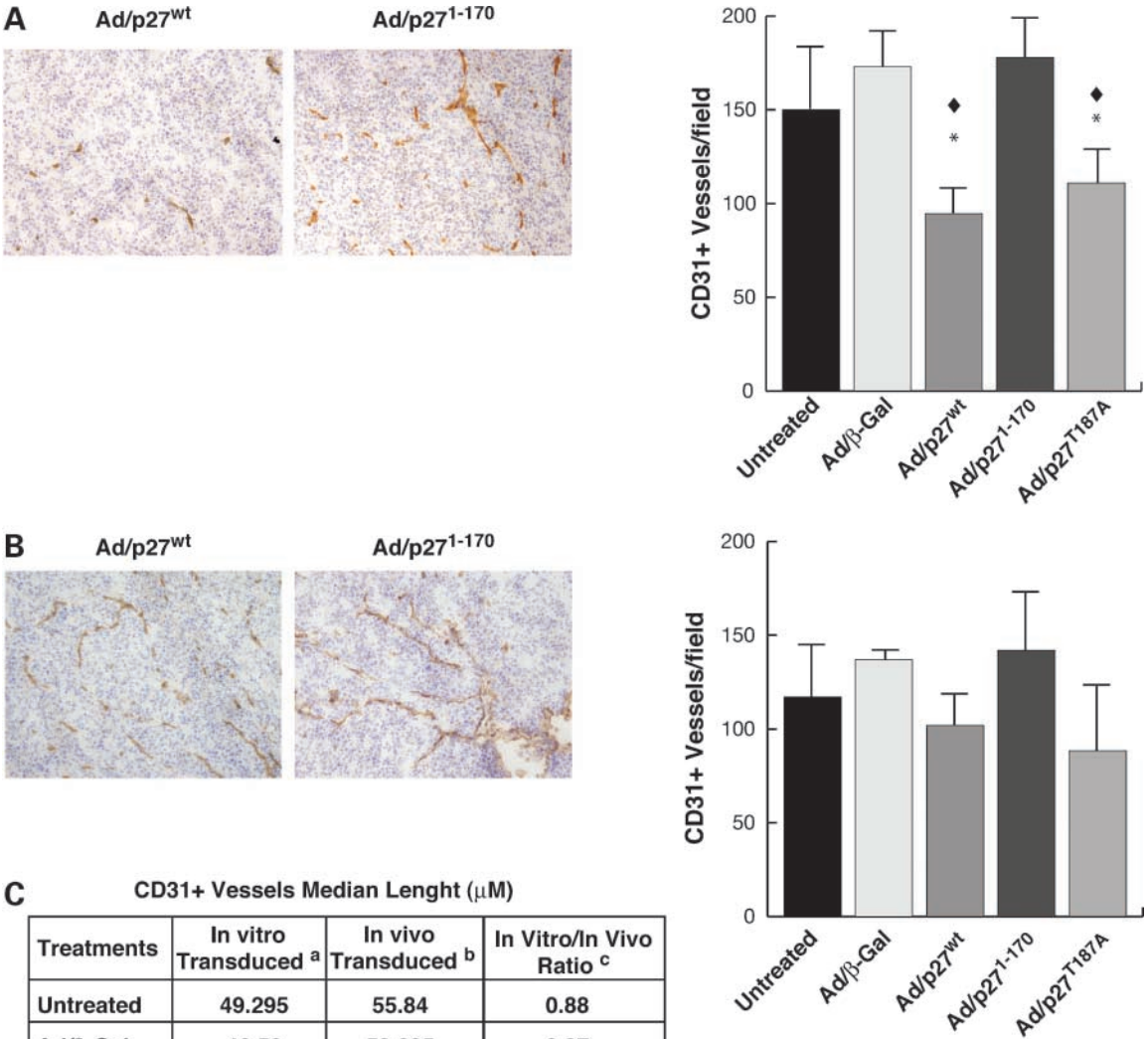

C CD31+ Vessels Median Lenght (μM)

Treatments	In vitro Transduced [a]	In vivo Transduced [b]	In Vitro/In Vivo Ratio [c]
Untreated	49.295	55.84	0.88
Ad/β-Gal	46.59	53.295	0.87
Ad/p27wt	57.275	26.98 *	2.12
Ad/p271-170	37.75	40.94 **	0.92
Ad/p27T187A	55.38	26.62 *	2.08

* p < 0.0001 vs Untreated, Ad/β-Gal and Ad/p27$^{1-170}$;
**p = 0.01 vs Untreated, or Ad/β-Gal

Figure 5. p27 inhibits tumor neoangiogenesis. Typical images of tumors treated with intratumoral injection of the indicated adenoviruses (**A**, *left*) or formed from pretransduced cells (**B**, *left*) and stained with the anti-CD31 (PECAM) antibody (*brown*). Magnification, ×250. Quantification of vessel densities per field in tumors treated as indicated by intratumoral injection (**A**, *right*) or formed from pretransduced cells (**B**, *right*). Microvessel density in AdTRE p27^{wt} and p27^{T187A}-treated tumors was reduced by 37% compared with untreated tumors. *, $P < 0.05$ versus untreated; ♦, $P < 0.01$ versus p27$^{1-170}$-treated and versus AdTRE β-Gal-treated tumors as calculated by Student's *t* test. **C,** comparative analysis of vessel median length in tumors formed from pretransduced cells (*a*) or treated with adenoviral intratumoral injections (*b*). *c,* median vessel length ratio obtained by dividing for each treatment the value in *column a* by the value in *column b*. These data show that *in vivo* injection of p27^{wt} and p27^{T187A} protein results in 2-fold reduction of vessel length with respect to tumors formed from pretransduced cells. Statistical significance was obtained using the Student's *t* test.

least four sections per tumor were analyzed. For each treatment group, four different tumors were analyzed. Only vessels >10 μm in length were considered.

Migration Experiments

Adhesion and migration assays were done essentially as described previously (5, 27). Briefly, for migration, bottoms of HTS Fluoroblok (Becton Dickinson) were coated overnight at 4°C with 20 μg/mL fibronectin, 10 μg/mL vitronectin, 10 μg/mL collagen I, or 10 μg/mL collagen VI and then saturated 2 h at room temperature with PBS-1% bovine serum albumin. Cells were labeled with DiI (Molecular Probes) for 20 min at 37°C before being seeded

in the Fluoroblok upper chamber and then incubated at 37°C for the indicated times. Migrating cells were evaluated by reading at different time points the lower and upper sides of the membrane with the Spectrafluor reader (Tecan). Each experiment was done at least three times in duplicate. In some experiments, migration was blocked at the indicated time point, by fixing the Fluoroblok membranes in 4% paraformaldehyde and the Fluoroblok membrane mounted on a slide, to allow the count of migrated cells.

For three-dimensional Matrigel evasion assay, cells (3×10^5/mL) were transduced as indicated and 48 h later were included in Matrigel (6 mg/mL; Becton Dickinson) or collagen I (1 mg/mL; Becton Dickinson) drops and incubated for the indicated times in complete medium. Cell motility was observed by transmission microscopy using a Nikon TS100/F microscope. Images were collected using a digital camera (Nikon).

For three-dimensional Matrigel invasion assay, glioblastoma cells were transduced as indicated and 48 h later seeded in the Fluoroblok upper chamber coated with 80 μg/mL Matrigel and then incubated at 37°C for 2 days. Fluoroblok membranes were then fixed in 4% paraformaldehyde, cells were stained with propidium iodide as indicate above, and the Fluoroblok membranes were mounted on a slide to allow the count of migrated cells.

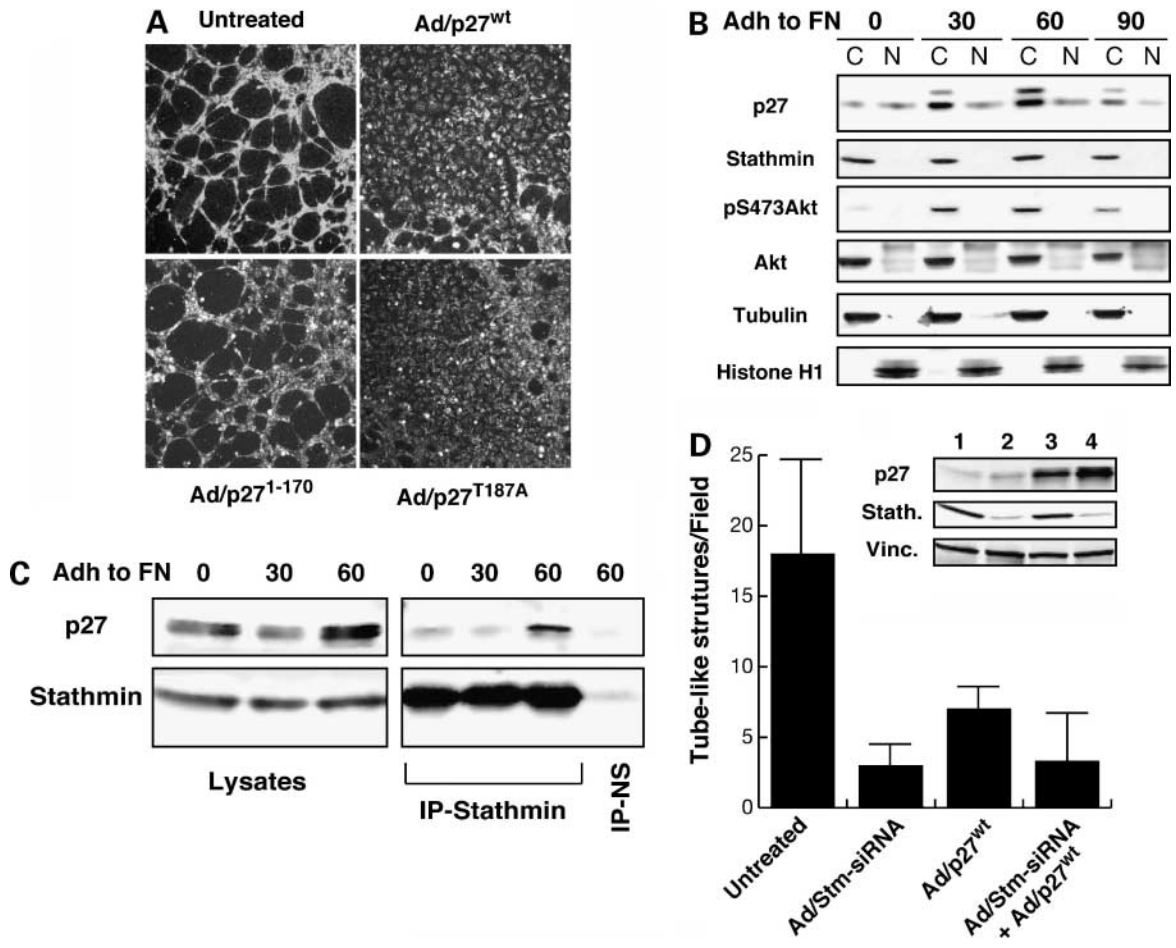

Figure 6. p27 impairs endothelial cell motility through stathmin. **A,** typical images formed by HUVEC transduced as indicated and 2 d later plated on Matrigel and incubated for 2 h in U87MG conditioned medium. Magnification, ×200. **B,** HUVEC were adhered to fibronectin-coated plates and at the indicated times cytoplasmic/nuclear extracts (*C/N*) were prepared and analyzed in Western blot analysis for p27 and stathmin expression. Tubulin and histone H1 expression were used as controls for the cytoplasmic fractions and nuclear purity and loading fractions, respectively. Adhesion-dependent activation of AKT visualized using a phosphospecific antibody directed against its phosphorylated Ser^{473} was used to confirm the activation of intracellular pathways due to cell-ECM contact. An adhesion-dependent cytoplasmic shift of p27 is observed after 30 and 60 min of adhesion. **C,** expression of endogenous p27 and stathmin in cytoplasmic extracts of HUVEC serum starved (0 min) and then adhered to fibronectin for 30 and 60 min and in the same extracts immunoprecipitated with an anti-stathmin antibody. *IP-NS,* immunoprecipitation done with a nonspecific rabbit IgG. **D,** number of tube-like structures per field (magnification, ×200) formed by HUVEC transduced with the indicated adenovirus and 3 d later plated on Matrigel and incubated for 2 h in U87MG conditioned medium. Mean ± SD of two independent experiments in which 10 different randomly selected fields were counted. *Inset,* expression of stathmin and p27 in HUVEC used in a typical experiment. *Lane 1,* untreated cells; *lanes 2* to *4,* cells were transduced with the indicated adenovirus: *2,* Ad/stathmin siRNA; *3,* Ad/TRE $p27^{wt}$; *4,* Ad/TRE $p27^{wt}$ + Ad/stathmin siRNA.

At least 10 randomly selected fields per membrane were counted in two different experiments done in duplicate.

Tube Formation Assay

HUVEC were transduced using a 60:30 recombinant AdTRE/AdTet-ON in the presence of 1.0 μg/mL doxycycline 48 h before seeding on Matrigel (BD PharMingen; 12.9 mg/mL)–coated LabTek (55,000 cells per chamber) and incubated for 2 h with normal growth medium or U87 conditioned medium. In some experiments, HUVEC were also transduced with Ad/stathmin small interfering RNA (siRNA) at multiplicity of infection 500 and 24 h later with AdTRE $p27^{wt}$ as described above. Nontransduced HUVEC were used as control. Results are expressed as number of tube-like structures per field (magnification, ×200).

The others methods used in this work are fully described in the Supplementary Material.[6]

Results

Cytoplasmic p27 Expression Correlates with Glioblastoma Cell Motility

To study the role of p27 in human glioblastoma, p27 expression and localization was evaluated in 10 different glioblastoma cell lines by Western blot. Except for T98G cells, p27 is generally expressed at low levels in the analyzed glioblastoma cell lines (Fig. 1A, *left*). Differential extraction of cytoplasmic and nuclear proteins showed that in the majority of these cell lines p27 presented an enriched nuclear localization, although some protein was also present in the cytoplasm (Supplementary Fig. S1B).[6] A comparison of only the cytoplasmic fractions revealed that in U251 and SBN75 cell lines p27 was almost completely absent, whereas two cell lines, T98G and U138MG, expressed high levels of cytoplasmic p27 (Fig. 1A, *right*). The analysis of p27 expression and localization by immunohistochemistry on a small panel of primary human brain tumors confirmed the results obtained on cell lines showing that high-grade brain tumors express low levels of p27 protein. In fact, all glioblastoma cases ($n = 4$) showed a lower expression of p27 compared with anaplastic astrocytoma ($n = 4$; Supplementary Fig. S1A).[6] In both types of tumors, p27 staining was predominantly nuclear.

To assess if the different cellular localization of p27 could be associated to differences in the growth rate and/or ECM-driven cell motility, proliferation and migration assays were done on four representative cell lines: T98G and U138MG cells displaying strong cytoplasmic p27 expression and U87MG and SF268 displaying low cytoplasmic levels. Results showed that no direct correlation could be established between cytoplasmic levels of p27 and proliferation rates (Fig. 1B), whereas T98G and U138MG cells, which had strong p27 cytoplasmic expression, exhibited a decreased migration rate through collagen IV (Fig. 1C), vitronectin, collagen I (Supplementary Fig. S1C),[6] and fibronectin (Fig. 2; data not shown) compared with SF268 and U87MG cells that expressed low cytoplasmic p27 levels.

Effects of p27 on Glioblastoma Cell Growth and Motility

We showed previously that a p27 deletion mutant lacking the last 28 amino acids ($p27^{1-170}$) retains the growth inhibition ability while failing to inhibit cell motility through ECM substrates (5). Based on this notion and to determine the effects of p27 overexpression on growth and motility of glioblastoma cells, different recombinant adenoviruses (AdTRE) were prepared expressing $p27^{wt}$, $p27^{1-170}$, and $p27^{T187A}$ (see Supplementary Material).[6] This last protein carries a point mutation resulting in the substitution of threonine 187 with alanine, which in turn impairs p27 degradation via the ubiquitin-dependent proteasome pathway (28, 29), thus representing a better control of the $p27^{1-170}$ mutant than the wild-type protein, because it also lacks the T187. Standardization of this expression system for different glioblastoma cells is described in Supplementary Fig. S2.[6] It consisted in determining the most suitable cotransduction ratio and doxycycline concentration to achieve a good inducible protein expression in at least 80% of transduced cells. As a control, AdTRE β-Gal (able to express the β-galactosidase protein on induction with doxycycline) was used. In all the cell lines tested, similar expression of the three p27 proteins was obtained (Supplementary Fig. S2; data not shown).[6] Biological characterization of p27 overexpression on cell growth was done on U87MG and U251MG. The three adenoviruses were able to inhibit *in vitro* proliferation of both cell lines with a similar profile as shown by cell growth curve (Supplementary Fig. S3A)[6] and fluorescence-activated cell sorting analysis of DNA content (Supplementary Fig. S3B).[6] In long-term growth assay (that is, colony assay), all the adenoviruses were able to significantly impair cell growth, although AdTRE $p27^{1-170}$ was the most effective one (Supplementary Fig. S3C).[6]

To determine the effects of the different p27 proteins on glioblastoma cell motility, U87MG and U251MG cells were transduced with the AdTRE p27/AdTet-ON and then tested in migration experiments on FN (Fig. 2A). Overexpression of $p27^{wt}$ and $p27^{T187A}$ induced a significant impairment of U87MG cell migration (65% and 67.5% of inhibition, respectively), whereas $p27^{1-170}$ was much less effective (30% of migration inhibition; $P \leq 0.01$ versus $p27^{wt}$ and $p27^{T187A}$, Student's t test; Fig. 2A). Conversely, overexpression of p27 did not alter the migration pattern of U251MG cells (Fig. 2B). In agreement with the above results, $p27^{wt}$ and $p27^{T187A}$ inhibited U87MG cell motility also in other migration assays, evaluating cell movements under three-dimensional conditions (Fig. 2C and D). Again, $p27^{1-170}$ failed to properly inhibit cell migration in both types of assays, confirming that the COOH-terminal portion of p27 is required to fully inhibit ECM-driven cell motility (5). Also in the three-dimensional experiments, U251 cells transduced with the three AdTRE p27 migrated

[6] Supplementary material for this article is available at Molecular Cancer Therapeutics Online (http://mct.aacrjournals.org/).

at a similar rate (data not shown). To understand the molecular basis of this different biological behavior, we first investigated the localization of endogenous and overexpressed p27 proteins in U87MG and U251MG cells adhered to fibronectin for 1 h. U87MG cells showed a predominant cytoplasmic localization in either nontransduced or transduced cells as evaluated by Western blot and immunofluorescence analysis (Fig. 3A and B). In contrast, in U251MG cells, p27 mainly localized in the nuclear compartment (Fig. 3). Western blot analysis revealed that, albeit very small, a fraction of overexpressed protein is also present in the cytoplasm of U251MG cells, but it is mainly cleaved at its COOH terminus as revealed using antibodies recognizing the COOH terminus (C19) or NH_2 terminus of p27 protein (N20; Fig. 3A, *right*). The caspase inhibitor Z-VAD -FMK almost completely prevented p27 cytoplasmic degradation (Fig. 3C), suggesting that the cytoplasmic cleavage of p27 in U251MG cells is dependent on caspase activity.

Doxycycline-regulated p27 expression impairs glioblastoma growth and invasion *in vivo*. To verify whether *in vivo* the various AdTRE p27 were able to inhibit glioblastoma cell growth, U87MG cells, known to be able to grow when implanted s.c. in nude mice, were used. On the contrary, U251MG cells could not be used because they are unable to form tumors in the same type of assay (30). U87MG xenografts were established using pretransduced cells and their growth was followed in animals fed with doxycycline. As controls, untreated and AdTRE β-Gal-transduced cells were used. From all controls, we obtained similar results (Fig. 4A; data not shown) and Western blot analysis showed that also *in vivo* the transgene expression was regulated by doxycycline (Fig. 4B, *right*; data not shown). In this experiment, AdTRE $p27^{1\text{-}170}$ transduction was the most effective in growth inhibition (60%), whereas $p27^{wt}$ and $p27^{T187A}$ overexpression gave 43% and 54% of tumor growth inhibition, respectively, in line with the *in vitro* experiments (Supplementary Fig. S3C).[6] These data showed that p27 overexpression is able to reduce glioblastoma cell growth *in vivo*.

Next, we asked whether the various AdTRE p27 could be used to treat glioblastoma *in vivo*. To this aim, U87MG xenografts tumors were established in nude mice by s.c. injection. Tumor treatments, consisting of five intratumoral injections of the various AdTRE p27, started as the tumors reached the volume of ~50 mm^3 (Fig. 4B, *left*). In a pilot experiment (n = 3 mice per group of treatment), mice transduced with AdTRE $p27^{wt}$ and AdTRE $p27^{1\text{-}170}$ were fed or not with doxycycline and the tumor growth was evaluated every 3 days up to 24 days after injection unless noted. Induction of p27 expression by doxycycline treatment (Fig. 4B, *right*) reduced tumor growth and increased the survival of mice of ~10 days (Fig. 4B, *left*), showing that growth inhibition was specifically due to p27 expression and not to adenoviral transduction. In a larger experiment (n = 8-10 mice per group of treatment), all AdTRE p27 tested significantly inhibited U87MG growth (Fig. 4C, *left*) compared with untreated and AdTRE β-Gal-transduced tumors. When tumor growth inhibition was evaluated using the tumor weight as a variable, a significantly stronger activity was observed for AdTRE $p27^{wt}$ and $p27^{T187A}$ compared with AdTRE $p27^{1\text{-}170}$ (60% and 70% versus 45% of tumor growth inhibition, respectively; Fig. 4C, *left*).

Histologic analysis of explanted tumors was carried out to search for signs of local invasion. Samples were judged as positive when at least two foci per section of invasive growth were found. Interestingly, we found that only one of seven different AdTRE $p27^{wt}$-treated tumors exhibited signs of local invasion (12.5%; Fig. 4C, *right*), whereas untreated and AdTRE $p27^{1\text{-}170}$-treated tumors showed a local invasion in 57% and 60% of cases, respectively.

p27 inhibition of cell invasion was linked to its ability to bind the microtubule-destabilizing protein stathmin (5). Accordingly, in tumors treated with AdTRE $p27^{wt}$, but not with AdTRE $p27^{1\text{-}170}$, stathmin coprecipitated with the transduced protein (Fig. 4D), whereas the two proteins similarly bound to cyclin/cyclin-dependent kinase complexes (Supplementary Fig. S3D-F; data not shown).[6] Overall, these data showed that intratumoral gene therapy approach based on p27 overexpression is able to significantly inhibit glioblastoma cell growth and invasion and that the COOH-terminal portion of p27 is necessary for the proper p27 activity *in vivo*.

p27 Expression Affects Tumor Vascularization

The data collected using the intratumoral treatment were in apparent contrast with the tumor growth inhibition observed when U87MG cells were transduced with the various AdTRE p27 before tumor cell injection in nude mice. In this type of experiment, in fact, AdTRE $p27^{1\text{-}170}$ showed the strongest tumor growth inhibition, in accord with *in vitro* experiments. Thus, we speculated that intratumoral injections of AdTRE p27 could function not only on cancer cells but also by altering the tumor microenvironment. This hypothesis was also supported by the fact that AdTRE $p27^{wt}$ and $p27^{T187A}$ exerted a higher growth-inhibitory activity when injected in preformed tumors with respect to when pretransduced in U87MG cells (compare Fig. 4A and C).

Previous works showed that inducible overexpression of $p27^{wt}$ and $p27^{T187A}$ in endothelial cells blocked DNA replication, inhibited cellular migration and tubulogenesis *in vitro*, and impaired angiogenesis in a mouse model of hind limb ischemia (7). Taking into account these results and our *in vivo* observations (Fig. 4), we investigated whether p27 overexpression had any effect on U87MG tumor neoangiogenesis. To this aim, we analyzed microvessel density in explanted tumors derived from the intratumoral or the pretransduced treatments using the anti-CD31 (PECAM) antibody. When AdTRE $p27^{wt}$ and $p27^{T187A}$ were administered intratumorally, they significantly reduced the number (Fig. 5A) and the length (Fig. 5C) of $CD31^+$ vessels with respect to control, AdTRE β-Gal, or AdTRE $p27^{1\text{-}170}$-treated tumors. Conversely, when the same analysis was carried on tumors formed by pretransduced cells, no significant difference was observed among the

treatments, and tumors formed by untreated or pretransduced U87MG cells presented similar vascularization (Fig. 5B and C). A semiquantitative proteomic analysis of U87MG conditioned medium derived from nontransduced and AdTRE $p27^{wt}$-transduced cells on 174 known cytokine showed no significant differences in the amount of proangiogenic factors produced by U87MG cells (Supplementary Table S1),[6] supporting the idea that the different tumor vascularization was due to a direct effect of p27 on mouse endothelial cells.

p27 Impairs Endothelial Cell Motility Through Stathmin

To dissect the role of p27 on tumor-induced angiogenesis, HUVEC were used as a model system. We first evaluated the effects of U87MG conditioned medium on HUVEC growth and motility, comparing it with the HUVEC standard growth medium. U87MG conditioned medium did not significantly stimulate HUVEC growth (data not shown) but profoundly increased their ability to form tube-like structures when cells were seeded on top of a Matrigel matrix (Supplementary Fig. S4A).[6]

Next, AdTRE p27 overexpression in HUVEC was standardized (Supplementary Fig. S4B-E).[6] Data showed that similar levels of protein expression were achieved using the three AdTRE p27 (Supplementary Fig. S3D)[6] and that, as expected, overexpression of $p27^{wt}$, $p27^{1-170}$, and $p27^{T187A}$ resulted in a similar proliferation inhibition (Supplementary Fig. S4E).[6] Then, the effect of $p27^{wt}$, $p27^{1-170}$, and $p27^{T187A}$ on HUVEC motility stimulated by U87MG conditioned medium was evaluated. $p27^{wt}$ and $p27^{T187A}$ significantly impaired tube-like structures formation by HUVEC (4.8 ± 2.1 and 5.5 ± 3 structures per field, respectively, with respect to 18 ± 8 of nontransduced cells; $P \leq 0.01$), whereas no significant difference was induced by $p27^{1-170}$ with respect to control cells (11 ± 4 versus 18 ± 8, respectively; $P = 0.2$; Fig. 6A). We described previously that the negative effects of p27 on sarcoma cell migration requires two fundamental modifications: the cytoplasmic localization of p27 in response to cell-ECM interaction and the consequent p27 binding to the microtubule-destabilizing protein stathmin (5). We thus verified whether in endothelial cells the same mechanism was functioning. Nucleocytoplasmic translocation of p27 was clearly observed in HUVEC after cell adhesion to fibronectin (Fig. 6B). Accordingly, an increased adhesion-dependent association between p27 and stathmin was observed by coimmunoprecipitation (Fig. 6C). These data support the hypothesis that p27 impairs HUVEC motility by inhibiting stathmin activity. To prove this point, we down-regulated stathmin in HUVEC using a specific siRNA. Inhibition of stathmin expression resulted in a strong inhibition of tube-like structures formation (Fig. 6D); more importantly, the overexpression of $p27^{wt}$ protein in stathmin silenced cells did not further inhibit HUVEC motility on Matrigel (Fig. 6D). This result suggests that stathmin expression is necessary for proper endothelial cell motility and that its association with p27 could be an important event in the regulation of endothelial cell motility both *in vitro* and *in vivo*. Accordingly, endogenous p27/stathmin colocalization was readily observed in cells forming tube-like structures on a three-dimensional Matrigel matrix as shown by the immunofluorescence analysis (Supplementary Fig. S4F).[6]

Discussion

Many previous works suggested that p27 could represent a proper candidate for targeted gene therapy in several types of cancer including glioblastoma (31–37), and our data support and expand our knowledge of the tumor-suppressive role of p27 *in vivo* at least in mice.

Our *in vitro* work showed that p27 is able to inhibit both cell growth and motility in glioblastoma cells. The latter effect depends on the COOH-terminal portion of the protein and on its cytoplasmic displacement as supported by several evidences presented here. (*a*) The analysis of p27 expression and localization coupled with motility and proliferation experiments in different glioblastoma cell lines (Fig. 1; Supplementary Fig. S1)[6] support the concept that p27 inhibits cell growth when located into the cell nucleus, whereas the control of cell motility is to ascribe to its cytoplasmic pool. (*b*) In U87MG cells, cytoplasmic p27 expression inhibits motility through its COOH-terminal portion (Figs. 2 and 3). (*c*) In U251MG cells, p27 overexpression did not interfere with cell motility probably due to the fact that in these cells p27 is retained in the nucleus and is cleaved at its COOH terminus by caspase activity (Fig. 3). Previous work showed that caspase are able to cleave p27 and p21 (38), although its significance for p27 was not assessed. Our data showed that in U251MG cells cleavage of p27 occurs at high rate in the cytoplasm, suggesting that several mechanisms control p27 expression, localization, and activity in glioblastoma cells.

Here, we provide the first demonstration that p27/stathmin interaction plays a pivotal role in the control of tumor cell invasion in *in vivo* models, confirming our previous results using *in vitro* experiments (5). Accordingly, recent data suggest that the knockout of p27 in human mammary carcinoma cells results in increased cell growth and motility (39), supporting again its tumor-suppressive role, at least in human cancer cells. However, a protumorigenic role for p27 has been recently shown in mice (40); however, whether the ''oncogenic'' activity of p27 depend on its cytoplasmic or nuclear part is still to be determined and whether it is dependent on its role in the control of cell motility is similarly unexplored (41).

The use of different mutants allowed us to show that p27 may also play important roles in the control of tumor microenvironment modification, specifically inhibiting tumor-induced neoangiogenesis. At least part of the effects exerted by p27 seems to be mediated by its interaction with stathmin in the cytoplasm of tumor and endothelial cells. This was shown either by the use of a deletion mutant unable to bind stathmin or by the use of a siRNA approach on HUVEC. It is increasingly clear that modulation of microtubule dynamics plays an important role in the regulation of several aspects of cell physiology, including cell motility (42). Thus, it is not surprising that interfering

with stathmin activity can result in the alteration of several aspects of the cell physiology. Accordingly, Atweh et al. recently confirmed a prominent role for stathmin in the control of HUVEC motility (43), thus independently confirming our finding.

Previous work on U87MG cells injected in nude mice showed that these cells locally invaded the surrounding tissues and suggested that stable p27 silencing could impair this effect (44). We therefore tried to inhibit p27 expression in U87MG cells using our adenoviral siRNA system. None of the tested siRNA (included the one used by Wu et al.) was able to significantly reduce p27 levels in these cells (Supplementary Fig. S5),[6] suggesting that other mechanisms, linked with cell clones selection, could be responsible for the reported effects in that study. Other studies suggested that the effects of p27 on cell motility could be due to the inhibition of the RhoA-ROCK pathway (6, 44). It is increasingly clear that RhoA hyperactivation inhibits two-dimensional motility, e.g., when wound healing or two-dimensional random motility assays are used, whereas it increases cell migration and invasion when the cells are tested in a three-dimensional context and *in vivo* (45–48). Moreover, several observations suggest that altering the microtubule network results in altered RhoA activity and/or localization, which in turn could contribute to altered cell motility (reviewed in ref. 49). Thus, it is conceivable that p27 could indirectly contribute to regulating RhoA activity through its interaction with stathmin and the consequent modulation of microtubule dynamics. Indeed, several experimental evidences produced in our laboratory support this hypothesis.[7]

In summary, we report here that, at least in glioblastoma, p27-based gene therapy could represent a promising approach and provide evidence that its tumor-suppressive activity is due not only to block of cell proliferation but also to tumor microenvironment modification, opening new way to look at gene therapy approach in human cancer.

Disclosure of Potential Conflicts of Interest

No potential conflicts of interest were disclosed.

Acknowledgments

We thank Sara D'Andrea for excellent technical assistance.

[7] Belletti et al., in preparation.

References

1. Sherr CJ, Roberts JM. CDK inhibitors: positive and negative regulators of G1-phase progression. Genes Dev 1999;13:1501 – 12.

2. Baldassarre G, Belletti B, Bruni P, et al. Overexpressed cyclin D3 contributes to retaining the growth inhibitor p27 in the cytoplasm of thyroid tumor cells. J Clin Invest 1999;104:865 – 74.

3. Blain SW, Scher HI, Cordon-Cardo C, Koff A. p27 as a target for cancer therapeutics. Cancer Cell 2003;3:111 – 5.

4. Rodier G, Montagnoli A, Di Marcotullio L, et al. p27 cytoplasmic localization is regulated by phosphorylation on Ser^{10} and is not a prerequisite for its proteolysis. EMBO J 2001;20:6672 – 82.

5. Baldassarre G, Belletti B, Nicoloso MS, et al. p27(Kip1)-stathmin interaction influences sarcoma cell migration and invasion. Cancer Cell 2005;7:51 – 63.

6. Besson A, Gurian-West M, Schmidt A, Hall A, Roberts JM. $p27^{Kip1}$ modulates cell migration through the regulation of RhoA activation. Genes Dev 2004;18:862 – 76.

7. Goukassian D, Diez-Juan A, Asahara T, et al. Overexpression of p27(Kip1) by doxycycline-regulated adenoviral vectors inhibits endothelial cell proliferation and migration and impairs angiogenesis. FASEB J 2001; 15:1877 – 85.

8. McAllister SS, Becker-Hapak M, Pintucci G, Pagano M, Dowdy SF. Novel p27(kip1) C-terminal scatter domain mediates Rac-dependent cell migration independent of cell cycle arrest functions. Mol Cell Biol 2003; 23:216 – 28.

9. Sun J, Marx SO, Chen HJ, Poon M, Marks AR, Rabbani LE. Role for p27(Kip1) in vascular smooth muscle cell migration. Circulation 2001; 103:2967 – 72.

10. Belletti B, Nicoloso MS, Schiappacassi M, et al. p27(kip1) functional regulation in human cancer: a potential target for therapeutic designs. Curr Med Chem 2005;12:1589 – 605.

11. Malumbres M, Barbacid M. To cycle or not to cycle: a critical decision in cancer. Nat Rev Cancer 2001;1:222 – 31.

12. Lacoste-Collin L, Gomez-Brouchet A, Escourrou G, Delisle MB, Levade T, Uro-Coste E. Expression of p27(Kip1) in bladder cancers: immunohistochemical study and prognostic value in a series of 95 cases. Cancer Lett 2002;186:115 – 20.

13. Mineta H, Miura K, Suzuki I, et al. p27 expression correlates with prognosis in patients with hypopharyngeal cancer. Anticancer Res 1999a; 19:4407 – 12.

14. Mineta H, Miura K, Suzuki I, et al. Low p27 expression correlates with poor prognosis for patients with oral tongue squamous cell carcinoma. Cancer 1999;85:1011 – 7.

15. Rabbani F, Koppie TM, Charytonowicz E, Drobnjak M, Bochner BH, Cordon-Cardo C. Prognostic significance of $p27^{Kip1}$ expression in bladder cancer. BJU Int 2007;100:259 – 63.

16. Thomas GV, Szigeti K, Murphy M, Draetta G, Pagano M, Loda M. Down-regulation of p27 is associated with development of colorectal adenocarcinoma metastases. Am J Pathol 1998;153:681 – 7.

17. Tsihlias J, Kapusta LR, DeBoer G, et al. Loss of cyclin-dependent kinase inhibitor $p27^{Kip1}$ is a novel prognostic factor in localized human prostate adenocarcinoma. Cancer Res 1998;58:542 – 8.

18. Liang J, Zubovitz J, Petrocelli T, et al. PKB/Akt phosphorylates p27, impairs nuclear import of p27 and opposes p27-mediated G_1 arrest. Nat Med 2002;8:1153 – 60.

19. Kirla RM, Haapasalo HK, Kalimo H, Salminen EK. Low expression of p27 indicates a poor prognosis in patients with high-grade astrocytomas. Cancer 2003;97:644 – 8.

20. Mizumatsu S, Tamiya T, Ono Y, et al. Expression of cell cycle regulator $p27^{Kip1}$ is correlated with survival of patients with astrocytoma. Clin Cancer Res 1999;5:551 – 7.

21. Piva R, Cavalla P, Bortolotto S, Cordera S, Richiardi P, Schiffer D. p27/kip1 expression in human astrocytic gliomas. Neurosci Lett 1997; 234:127 – 30.

22. Tamiya T, Mizumatsu S, Ono Y, et al. High cyclin E/low $p27^{Kip1}$ expression is associated with poor prognosis in astrocytomas. Acta Neuropathol 2001;101:334 – 40.

23. Nakasu S, Nakajima M, Handa J. Anomalous p27kip1 expression in a subset of malignant gliomas. Brain Tumor Pathol 1999;16:17 – 21.

24. Naumann U, Weit S, Rieger L, Meyermann R, Weller M. p27 modulates cell cycle progression and chemosensitivity in human malignant glioma. Biochem Biophys Res Commun 1999;261:890 – 6.

25. Zagzag D, Blanco C, Friedlander DR, Miller DC, Newcomb EW. Expression of p27KIP1 in human gliomas: relationship between tumor grade, proliferation index, and patient survival. Hum Pathol 2003;34: 48 – 53.

26. Jaffe EA, Nachman RL, Becker CG, Minick CR. Synthesis of antihemophilic factor antigen by cultured human endothelial cells. J Clin Invest 1973;52:2745 – 56.

27. Spessotto P, Giacomello E, Perris R. Improving fluorescence-based assays for the *in vitro* analysis of cell adhesion and migration. Mol Biotechnol 2002;20:285 – 304.

28. Montagnoli A, Fiore F, Eytan E, et al. Ubiquitination of p27 is regulated by Cdk-dependent phosphorylation and trimeric complex formation. Genes Dev 1999;13:1181 – 9.

29. Vlach J, Hennecke S, Amati B. Phosphorylation-dependent degradation of the cyclin-dependent kinase inhibitor p27. EMBO J 1997;16: 5334 – 44.

30. Ke LD, Shi YX, Yung WK. VEGF(121), VEGF(165) overexpression enhances tumorigenicity in U251 MG but not in NG-1 glioma cells. Cancer Res 2002;62:1854 – 61.

31. Katner AL, Gootam P, Hoang QB, Gnarra JR, Rayford W. Induction of cell cycle arrest and apoptosis in human prostate carcinoma cells by a recombinant adenovirus expressing p27(Kip1). J Urol 2002;168:766 – 73.

32. Koh TY, Park SW, Park K, et al. Inhibitory effect of p27KIP1 gene transfer on head and neck squamous cell carcinoma cell lines. Head Neck 2003;25:44 – 9.

33. Lee DW, Park SW, Park SY, Heo DS, Kim KH, Sung MW. Effects of p53 or p27 overexpression on cyclooxygenase-2 gene expression in head and neck squamous cell carcinoma cell lines. Head Neck 2004;26:706 – 15.

34. Matsunobu T, Tanaka K, Matsumoto Y, et al. The prognostic and therapeutic relevance of p27kip1 in Ewing's family tumors. Clin Cancer Res 2004;10:1003 – 12.

35. Park KH, Seol JY, Yoo C, et al. Adenovirus expressing p27(Kip1) induces growth arrest of lung cancer cell lines and suppresses the growth of established lung cancer xenografts. Lung Cancer 2001a;31:149 – 55.

36. Park KH, Seol JY, Kim TY, et al. An adenovirus expressing mutant p27 showed more potent antitumor effects than adenovirus-p27 wild type. Cancer Res 2001b;61:6163 – 9.

37. Park KH, Lee J, Yoo CG, et al. Application of p27 gene therapy for human malignant glioma potentiated by using mutant p27. J Neurosurg 2004;101:505 – 10.

38. Levkau B, Koyama H, Raines EW, et al. Cleavage of p21Cip1/Waf1 and p27Kip1 mediates apoptosis in endothelial cells through activation of Cdk2: role of a caspase cascade. Mol Cell 1998;1:553 – 63.

39. Yuan Y, Qin L, Liu D, et al. Genetic screening reveals an essential role of $p27^{kip1}$ in restriction of breast cancer progression. Cancer Res 2007;67: 8032 – 42.

40. Besson A, Hwang HC, Cicero S, et al. Discovery of an oncogenic activity in p27Kip1 that causes stem cell expansion and a multiple tumor phenotype. Genes Dev 2007;21:1731 – 46.

41. Sicinski P, Zacharek S, Kim C. Duality of $p27^{Kip1}$ function in tumorigenesis. Genes Dev 2007;21:1703 – 6.

42. Etienne-Manneville S. Actin and microtubules in cell motility: which one is in control? Traffic 2004;5:470 – 7.

43. Mistry SJ, Bank A, Atweh GF. Synergistic antiangiogenic effects of stathmin inhibition and Taxol exposure. Mol Cancer Res 2007;5:773 – 82.

44. Wu FY, Wang SE, Sanders ME, et al. Reduction of cytosolic p27(Kip1) inhibits cancer cell motility, survival, and tumorigenicity. Cancer Res 2006;66:2162 – 72.

45. Croft DR, Sahai E, Mavria G, et al. Conditional ROCK activation *in vivo* induces tumor cell dissemination and angiogenesis. Cancer Res 2004;64:8994 – 9001.

46. Sahai E, Garcia-Medina R, Pouyssegur J, Vial E. Smurf1 regulates tumor cell plasticity and motility through degradation of RhoA leading to localized inhibition of contractility. J Cell Bio 2007;176:35 – 42.

47. Torka R, Thuma F, Herzog V, Kirfel G. ROCK signaling mediates the adoption of different modes of migration and invasion in human mammary epithelial tumor cells. Exp Cell Res 2006;312:3857 – 71.

48. Wyckoff JB, Pinner SE, Gschmeissner S, Condeelis JS, Sahai E. ROCK- and myosin-dependent matrix deformation enables protease-independent tumor-cell invasion *in vivo*. Curr Biol 2006;16:1515 – 23.

49. Basu R, Chang F. Shaping the actin cytoskeleton using microtubule tips. Curr Opin Cell Biol 2007;19:88 – 94.